Hot-phonon effects on electron transport in quantum wires

R. Mickevičius,[a] V. Mitin, G. Paulavičius, and V. Kochelap[b]
Department of Electrical and Computer Engineering, Wayne State University, Detroit, Michigan 48202

M. A. Stroscio and G. J. Iafrate
U.S. Army Research Office, P.O. Box 12211, Research Triangle Park, North Carolina 27709

(Received 22 May 1995; accepted for publication 6 August 1996)

Hot (nonequilibrium) phonon effects on electron transport in rectangular GaAs/AlAs quantum wires have been investigated by a self-consistent Monte Carlo simulation. Confinement and localization of optical phonons have been taken into account. We have demonstrated that at room temperature hot optical phonons lead to a significant increase in electron drift velocity. This hot-phonon drag effect is due to the strongly asymmetric nonequilibrium phonon distribution. As a result, phonon absorption for forward transitions (electron gains momentum along electric field) is enhanced, whereas absorption for backward transitions (electron gains momentum against electric field) is suppressed. At low temperatures diffusive heating of electrons by hot phonons dominates over hot-phonon drag and the electron drift velocity decreases. © *1996 American Institute of Physics.* [S0021-8979(96)09721-6]

I. INTRODUCTION

Nonequilibrium phonon populations (hot phonons) generated by hot-electron gases affect virtually all electronic phenomena in semiconductors (see, e.g., Ref. 1) including electron relaxation, transport, noise, impact ionization, and optical response. Of various theoretical approaches to the hot phonon problem (see, e.g., Refs. 1–6) the ensemble Monte Carlo method[4,5] is probably the most suitable for the time-dependent and strongly nonequilibrium case.

Recent Monte Carlo studies[7–9] of the dynamics of nonequilibrium electron-phonon systems in quasi-one-dimensional (1D) quantum wire (QWI) structures indicate that hot-phonon phenomena in such structures display unique peculiarities not existing in bulk semiconductors and quantum wells (QWs). As in bulk semiconductors and QWs, nonequilibrium phonon populations strongly affect hot-electron relaxation in QWIs, but their effect in QWIs is twofold: hot phonons increase electron cooling rates at the very initial relaxation stage and decrease them when quasiequilibrium between electron and phonon subsystems is reached. Unlike in bulk materials and QWs, nonequilibrium phonon buildup and their role in electron relaxation depend strongly on the shape of initial distribution of injected or photoexcited electrons. Although hot-phonon buildup in QWIs is considerably more pronounced than in bulk materials and QWs for the same equivalent electron concentrations, their influence on electron transport in QWIs has not yet been studied. Due to the 1D nature of optical phonons in QWIs (assuming that phonons are confined) nonequilibrium optical phonons carry much of the directed momentum and their influence on electron transport should be quite pronounced.

In this paper we present self-consistent ensemble Monte Carlo simulations of electron transport in QWIs which include hot phonons.

[a]Electronic mail: vidas@neris.eng.wayne.edu
[b]Permanent address: Institute of Semiconductor Physics, National Academy of Sciences of Ukraine, Kiev, Ukraine.

II. MODEL AND METHOD

We have employed the ensemble Monte Carlo procedure[5] for the simulation of a coupled nonequilibrium electron-phonon system. We have considered GaAs/AlAs rectangular QWI with an infinitely deep potential well for electrons with multisubband parabolic band structure. Electron intersubband and intrasubband scattering by optical and acoustic phonons are considered. We have incorporated in our model optical phonon confinement within a QWI and localization at heterointerfaces.[10,11] Due to considerably stronger coupling with electrons in thick and moderate QWIs,[11] only nonequilibrium distributions of confined longitudinal optical (LO) phonons are taken into account. The distributions of two branches of surface optical (SO) (interface) phonons are assumed in equilibrium. Strong inelasticity of acoustic-phonon scattering[12] is also included in our model. We have considered rather high temperatures (30–300 K), and therefore electron-electron intersubband scattering and electron scattering by regions of interface roughness have been neglected. We have chosen the cross-section of the QWI of 150×250 Å^2. This moderately thick QWI has been chosen in order to diminish the role of acoustic-phonon scattering and the role or electron intersubband transitions. In thin QWIs, acoustic-phonon scattering is so strong that it largely determines electron relaxation and transport.[7] Hot-phonon buildup in QWIs is pronounced for electron concentrations n of the order of 10^5 cm^{-1} or more.[7,8] We have considered this electron concentration throughout our simulations.

1D systems have some peculiarities in nonequilibrium phonon buildup which must be carefully considered. Owing to optical phonon quantization and the resultant 1D momentum conservation in quantum wires, electrons can emit or absorb optical phonons with wave vectors which are strictly defined by the electron momentum and the phonon energy. In general, the phonon wave number is defined by the energy and momentum conservation equations and is given by

$$q=\sqrt{k^2+k'^2-2kk'\cos\theta}, \tag{1}$$

where k is the electron wave number before scattering, $k' = \sqrt{k^2 \pm 2m^*\omega_0/\hbar}$ is the electron wave number after absorption (sign +) or emission (sign −) of the optical phonon of frequency ω_0, and θ is the angle between electron wave vectors before and after scattering. In 1D structures there are just two final states for scattered electrons: forward scattering with $\cos\theta=1$, or backward scattering with $\cos\theta=-1$. Consequently, there are two possible phonon wave vectors available for emission (and two for absorption) by any single electron:

$$q_{\min}=|k-k'|, \quad q_{\max}=|k+k'|. \tag{2}$$

In contrast, in quantum wells (or bulk materials) due to existence of additional degree(s) of freedom, $\cos\theta$ can take any value in the range $(-1,+1)$, so that there is an entire range of phonon q values from $|k-k'|$ to $|k+k'|$ available for electron interactions. Therefore, electrons in QWIs having appreciably different energies generate nonequilibrium phonons in different, narrow q-space regions which do not overlap.

Nonequilibrium phonons have been included by calculating the phonon occupation number vs phonon wave vector (phonon distribution) within the Monte Carlo procedure. In accordance with the 1D nature of optical phonons in QWIs, the increment of a phonon occupation number after each emission (sign +) or absorption (sign −) event is given by the term $\pm(2\pi/\Delta q)\,(n/N)$, where Δq is the mesh step in q space used to record the N_q histogram, n is the linear electron concentration in a QWI, and N is the actual number of particles in the simulation.

In Monte Carlo simulations of bulk and 2D nonequilibrium electron-optical-phonon systems, the mesh step is not a crucial parameter, given that this step is much less than the q-space region populated by nonequilibrium phonons. Due to overlap of phonon distributions generated by various electrons in bulk and 2D systems [see Eq. (1)] the phonon reabsorption rate depends on the integrated (average) occupation number over the entire region which is not crucially sensitive to the mesh step. However, as we see from the above consideration, in 1D systems phonon distributions generated by electrons with different energies do not overlap, and the reabsorption rate depends only on the magnitude of the phonon occupation number N_q at an appropriate q value. Therefore, as the mesh step becomes smaller, both the occupation number at this particular q and the reabsorption rate become larger. There are, of course, physical limits on the magnitude of Δq. These limits follow from the uncertainty in the phonon longitudinal wave number due to the finite length of the QWI.

We have taken a QWI of length $L_x=10$ microns, so that $\Delta q=2\pi/L_x\approx 6\times10^3$ cm^{-1}. Hot-optical-phonon decay into acoustic phonons is taken into account by recalculating N_q for every mesh step at the end of each time step. For simulations we have used the bulk value of the optical phonon decay time $\tau_{\rm ph}=7$ ps, because the most complete existing model indicates that the decay time does not depend crucially on the dimensionality of the semiconductor structure.[13] The time step in our simulations has been chosen to be smaller than the average time between two events of electron scattering by optical phonons and much less than the phonon thermalization time $\tau_{\rm ph}$. We have not taken into account the increase in the acoustic phonon population as a result of the decay of nonequilibrium optical phonons. There are two reasons for this. First, the buildup of nonequilibrium optical phonons occurs only in a very narrow region of the Brillouin zone (near the zone center), so that over the entire zone the average occupation number increases only negligibly. This is true for systems of any dimensionality since the electrons interacting with phonons populate only the center region of the Brillouin zone. Second, the acoustic phonons in QWIs embedded in surrounding materials with similar elastic properties (GaAs in AlAs in our case) may penetrate through GaAs/AlAs interfaces and escape from the QWI. Therefore we have good thermal conductivity and the QWI should not be heated much more than the whole GaAs/AlAs structure. Given that the surrounding AlAs is sufficiently massive, the increase in temperature would be negligible even if the QWI strongly radiates acoustic phonons.

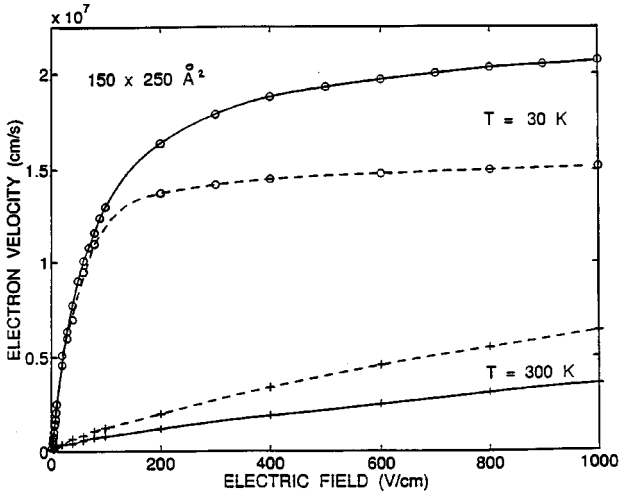

FIG. 1. Electron drift velocity as a function of electric field in QWI of cross-section 250×150 Å^2. Two upper curves are obtained for the equilibrium lattice temperature $T=30$ K, two lower curves for $T=300$ K. Solid curves are calculated without hot phonons, dashed curves with hot phonons.

III. HOT PHONONS IN A SINGLE QUANTUM WIRE

We have performed Monte Carlo simulations of electron transport in a single QWI under nonequilibrium phonon conditions. To reveal hot-phonon effects we have also calculated electron transport characteristics under equilibrium phonons.

Figure 1 illustrates the electron drift velocity as a function of applied electric field for two equilibrium lattice temperatures, $T=30$ K (two lower curves) and $T=300$ K (two lower curves). As one can see from Fig. 1, hot-phonon effects have opposite signs at low and high temperatures. At low temperatures, hot phonons reduce the electron drift velocity, while at high temperatures they increase it. The reason for this is as follows: Electron transport at low temperatures and with equilibrium phonons is close to streaming,[14–17] i.e., electrons accelerate with little scattering until they acquire the optical phonon energy, at which time they emit optical phonons and are scattered down to the sub-

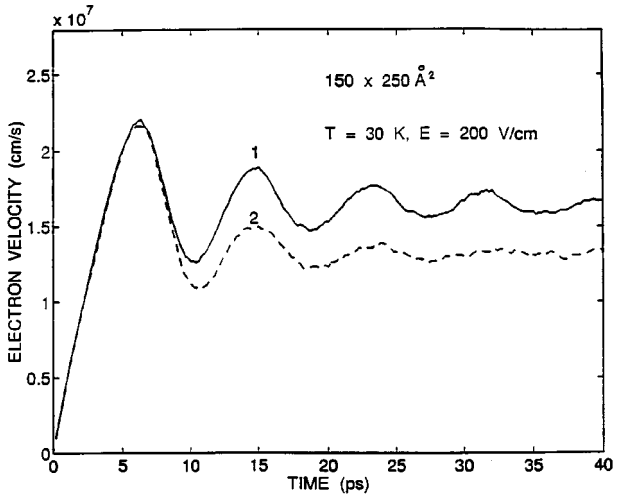

FIG. 2. Transient response of electron drift velocity to the electric field step $E=200$ V/cm. Solid curve 1 is obtained without hot phonons, dashed curve 2 with hot phonons. QWI: 250×150 Å^2, $T=30$ K.

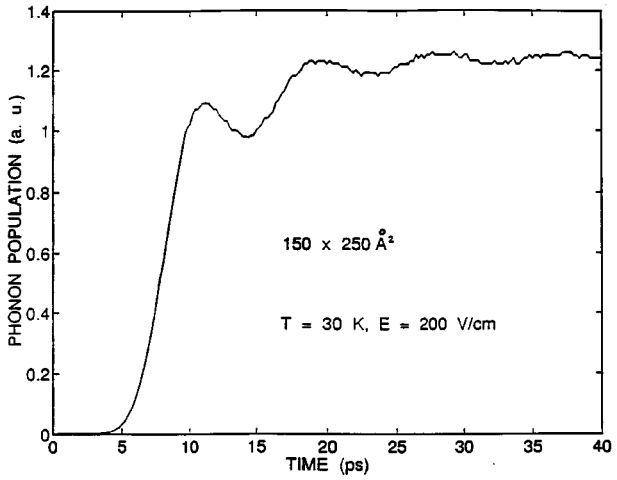

FIG. 3. Transient response of total phonon population to the electric field step $E=200$ V/cm. QWI: 250×150 Å^2, $T=30$ K.

band bottom. This process repeats periodically. In the streaming regime the electron drift velocity saturates at

$$v_s=\sqrt{\frac{\hbar\omega}{2m^*}}, \tag{3}$$

where $\hbar\omega$ is the optical phonon energy. Substituting numerical values for GaAs, we get $v_s\approx2.15\times10^7$ cm/s. Reabsorption of nonequilibrium optical phonons destroys the phase of electron motion and the streaming regime. As a result, electron drift velocity drops below the streaming velocity [Eq. (3)].

Figure 2 demonstrates the transient response of the electron drift velocity to an electric field step. One can see from Fig. 2 that drift-velocity oscillations due to streaming-like motion of electrons are effectively suppressed by hot phonons. Thus at low temperatures the hot-phonon effect is similar to the effect of lifting the equilibrium lattice temperature; hot phonons cause the randomization of electron momentum and increase in mean electron energy rather than the gain of directed momentum. Such a hot-phonon effect is called diffusive electron heating by hot phonons. Figure 3 shows the transient response of the total nonequilibrium phonon population (effective lattice temperature) in this near-streaming regime. Oscillations related to resonant periodic emission of optical phonons in the streaming regime are also quite pronounced.

The increase of electron drift velocity at a temperature of 300 K is related to the hot-phonon distribution in momentum space. Figures 4(a) and 4(b) illustrate the nonequilibrium LO phonon distributions at 1 kV/cm and $T=30$ K and 300 K, respectively. In both cases the phonon distribution is peaked in the forward direction. This peak is very sharp at low temperatures, whereas at high temperatures it is rather broad. (Sharp minima and maxima on this distribution are readily reproducible and, as discussed below, they correspond to various intrasubband and intersubband electron transitions with absorption or emission of LO phonon). One can see from Fig. 4(b) that at room temperature nonequilibrium pho-

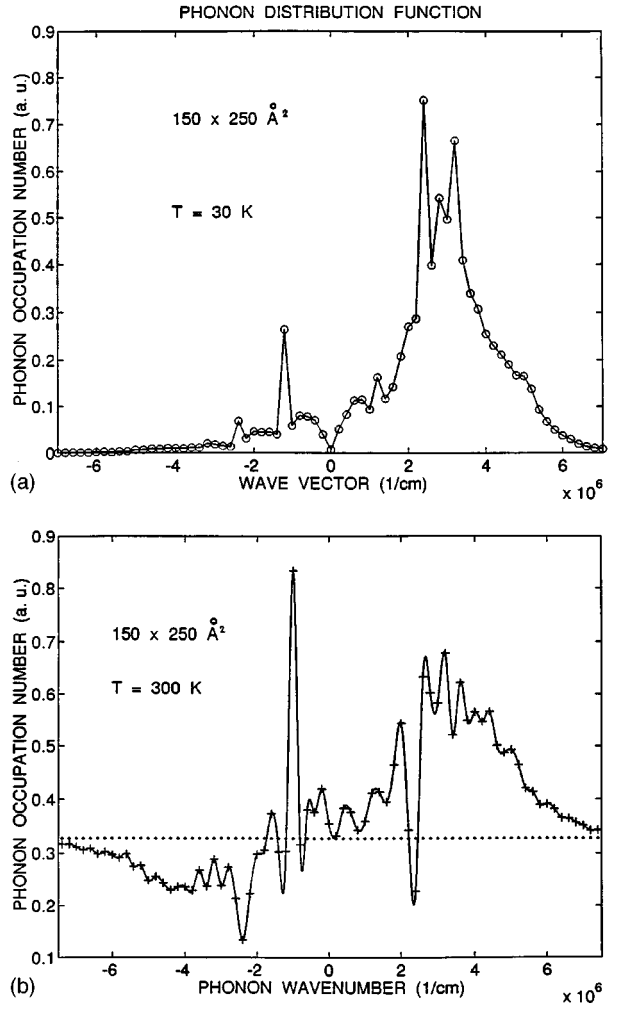

FIG. 4. Phonon occupation number vs phonon wave number for the same QWI as in Fig. 1 at two equilibrium lattice temperatures: (a) $T=30$ K and (b) $T=300$ K. Electric field is 1 kV/cm. Dotted line on part (b) represents the equilibrium phonon occupation number at 300 K.

non distribution displays not only a forward peak but also underpopulation of phonons at negative values of phonon wave number. Such a nonequilibrium phonon distribution is caused by the anisotropic electron distribution which occurs when electric fields are present; more electrons have positive momenta than negative ones. Electrons with positive momenta emit phonons with positive q, but can absorb phonons with either positive or negative wave numbers. Both the underpopulation of phonons with negative q and the overpopulation of phonons (hot phonons) with positive q cause the gain of directed momentum and are responsible for the enhancement of the electron drift velocity. Indeed, the underpopulation causes the suppression of electron scattering back in momentum space by the absorption of phonons. As a result, the electron distribution becomes more forward-peaked and the drift velocity increases. Phonon underpopulation has been theoretically obtained in bulk materials.[18] Due to the 3D nature of phonon wave vector in bulk crystals, this underpopulation has been weakly pronounced. Leo *et al.*[19–21] have measured experimentally the heating of cold electrons by warm lattice of a QW. Their experiments indicate that heating rate decreases when increasing electron concentration. This effect can be explained in terms of phonon underpopulation.[21] The gain of directed momentum due to the interaction with nonequilibrium phonons is usually called hot-phonon drag effect. Hot-phonon drag has been predicted in bulk materials (see, e.g., Ref. 3). However, due to weakly pronounced phonon underpopulation in bulk materials, this drag effect is small, unless the increase in mean electron energy leads to the suppression of strong ionized impurity scattering and a consequent increase in mobility.[22]

It must be noted that hot phonons in QWIs cause an increase in the mean electron energy. This increase is due to enhanced phonon absorption rates and is common for systems of arbitrary dimensionality and lattice temperature.

It should be pointed out that the simulation method proposed provides very valuable information about the coupled-electron and nonequilibrium optical-phonon system dynamics in the QWI structure. As Figs. 4(a) and 4(b) demonstrate, at different lattice temperatures the phonon spectra exhibit several characteristic features at specific values of the phonon wave vectors. These peaks and dips can be easily identified according to the momentum [Eqs. (1) and (2)] and the energy conservation in the case considered. In particular, it could be shown that for 30 K lattice temperature, the peaks at $q \approx \pm 2.3\times10^6$ cm^{-1} in Fig. 4(a) correspond to prevailing optical phonon emission by electrons in the lowest energetic subband when practically all the carrier energy is dissipated to these phonons. On the other hand, the dips at the same q locations for 300 K [see Fig. 4(b)] can be identified with dominant LO phonon absorption by ''slow'' electrons residing near the lowest subband bottom. The characteristic peak at $\approx -1.3\times10^6$ cm^{-1} in Figs. 4(a) and 4(b) is associated with the optical phonon emission by electrons in the second subband (located at $\approx$27 meV above the first subband). After the emission the carriers are scattered down to the lowest energetic subband. The above analysis demonstrates that the nonequilibrium phonon spectra reveal the change in the role of different electron-optical-phonon scattering ''channels'' in the QWI caused by changes in the lattice temperature or external electric field.

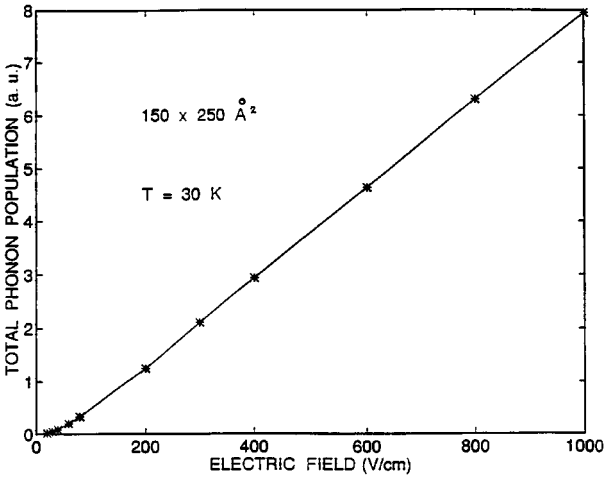

FIG. 5. Total phonon population as a function of electric field. QWI: 250 $\times$150 Å^2, T=30 K.

Figure 5 depicts the total phonon population plotted vs applied electric field. At fields exceeding 100 V/cm this dependence is essentially linear. The reason is that at higher fields in steady state the total power pumped into the electron system by the external electric field is dissipated via the emission of LO phonons. The total Joule power, $P_J = env_dE$, for the saturated drift velocity v_d is a linear function of electric field E. Therefore, the total phonon population which is proportional to P_J is also a linear function of E. The dependence is near exponential at low electric fields ($E<100$ V/cm).

IV. SUMMARY

By the ensemble Monte Carlo technique we have investigated electron transport under nonequilibrium phonon conditions in single, rectangular GaAs/AlAs quantum wires.

Let us list simplifications we have assumed in our model. We have not taken into account electron scattering by ionized impurities, regions of surface roughness, or electron-electron interactions. Although all these mechanisms may be very important at very low temperatures,[23,24] they are not of crucial importance for electron transport at T=30–300 K or at high electric fields. We have assumed infinitely deep potential wells for electrons. Under the transport conditions considered in this paper, a negligible fraction of electrons are heated above optical phonon energy (36.6 meV). The barrier height for GaAs/AlGaAs structures is of the order of several hundred of meVs so that such barriers may be considered as infinitely high under these transport conditions.

Our results have revealed twofold hot-phonon effects on electron transport in single QWIs. At low temperatures, diffusive heating of electrons by hot phonons prevails over hot-phonon drag effect and leads to the reduction of the electron drift velocity. At room temperature, due to the shifted forward electron distribution in momentum space, the nonequilibrium phonon population displays underpopulation at negative wave numbers and overpopulation (hot phonons) at

positive wave numbers. As a result, the rate of electron transitions back in momentum space assisted by phonon absorption are suppressed and transitions forward are enhanced. Hence, electron drift velocity as well as low-field mobility increase. This so-called hot-phonon drag effect is well pronounced in QWIs; the mobility and velocity increase by more than 30%.

It should be pointed out that the hot-phonon drag effect can find its application in a variety of novel nanoscale devices.[25]

[1] M. Lax and W. Cai, Int. J. Mod. Phys. B **6**, 171 (1992).
[2] P. Kocevar, Inst. Phys. Conf. Ser. **5**, 3349 (1972).
[3] P. Kocevar, Physica (Amsterdam) **134B**, 155 (1985).
[4] P. Lugli, C. Jacoboni, L. Reggiani, and P. Kocevar, Appl. Phys. Lett. **50**, 1251 (1987).
[5] R. Mickevičius and A. Reklaitis, Solid State Commun. **64**, 1305 (1987).
[6] L. Hlou, J. C. Vaissiere, J. P. Nougier, L. Varani, P. Houlet, L. Regiani, M. Fadel, and P. Kocevar, in Proceedings of the Third International Workshop on Comp. Electron, Portland, OR, 1994, p. 49.
[7] R. Gaška, R. Mickevičius, V. Mitin, M. A. Stroscio, G. J. Iafrate, and H. L. Grubin, J. Appl. Phys. **76**, 1 (1994).
[8] R. Mickevičius, R. Gaška, V. Mitin, M. A. Stroscio, and G. J. Iafrate, Semicond. Sci. Technol. **9**, 889 (1994).
[9] L. Rota, F. Rossi, P. Lugli, and E. Molinari, Semicond. Sci. Technol. **9**, 871 (1994).
[10] K. W. Kim, M. A. Stroscio, A. Bhatt, R. Mickevičius, and V. V. Mitin, J. Appl. Phys. **70**, 319 (1991).
[11] R. Mickevičius, V. V. Mitin, K. W. Kim, M. A. Stroscio, and G. J. Iafrate, J. Phys. Condens. Matter. **4**, 4959 (1992).
[12] R. Mickevičius and V. Mitin, Phys. Rev. B **48**, 17194 (1993).
[13] G. Mahler, A. M. Kriman, and D. K. Ferry (unpublished).
[14] R. Mickevičius, V. Mitin, U. K. Harithsa, D. Jovanovic, and J. P. Leburton, J. Appl. Phys. **75**, 973 (1994).
[15] W. Shockley, Bell Syst. Tech. J. **30**, 990 (1951).
[16] S. Komiyama, Adv. Phys. **31**, 255 (1982).
[17] D. Jovanovic and J. P. Leburton, Superlattices Microstruct. **11**, 141 (1992).
[18] P. Kocevar (private communication).
[19] K. Leo, W. W. Ruhle, and K. Ploog, Solid-State Electron. **32**, 1863 (1989).
[20] K. Leo, W. W. Ruhle, and K. Ploog, SSC **71**, 101 (1989).
[21] K. Leo (unpublished).
[22] R. Mickevičius and A. Reklaitis, J. Phys. Condens. Matter. **1**, 9401 (1989).
[23] J. P. G. Taylor, K. J. Hugill, D. D. Vvedensky, and A. MacKinnon, Phys. Rev. Lett. **67**, 2359 (1991).
[24] J. A. Nixon and J. H. Davies, Phys. Rev. B **41**, 7929 (1990).
[25] V. Mitin, V. Kochelap, R. Mickevičius, M. Dutta, and M. A. Stroscio (patent pending).